Crossover Leung-Griffiths Model and the Phase Behavior of Binary Mixtures With and Without Chemical Reaction[1]

M.Yu. Belyakov[a,b], S.B. Kiselev[a,b], and J.C. Rainwater[a]

[a] Physical and Chemical Properties Division
National Institute of Standards and Technology
325 Broadway, Boulder, Colorado 80303, USA

[b] Permanent address:
Institute for Oil and Gas Research of the Russian Academy of Sciences
Leninsky Prospect 63/2, Moscow 117917, Russia

[1] Draft, subject to revision.

Contribution of the National Institute of Standards and Technology,
not subject to copyright in the United States

May 28, 1997

ABSTRACT

A new theoretical crossover model for the phase behavior of binary mixtures is presented that corresponds to the Leung-Griffiths model in the critical region and is transformed into the regular classical expansion far away from the critical point. The model is optimized to, and leads to good agreement with, experimental vapor-liquid equilibrium data for CO_2 + n-butane, CO_2 + propane, ethane + benzene, CO_2 + methanol, and dilute aqueous solutions of NaCl in the extended critical region. Phase behavior of mixtures in the presence of chemical reaction and a possibility to incorporate this phenomenon into the model are also discussed.

KEY WORDS: benzene; binary mixtures; carbon dioxide; chemical reaction; critical phenomena; equation of state; ethane; methanol; n-butane; phase behavior; propane; sodium chloride; thermodynamic properties; water.

1. INTRODUCTION

The thermodynamic model for description of phase behavior of binary mixtures, first developed by Leung and Griffiths [1] and subsequently modified by Rainwater and co-workers [2], provides excellent correlations of experimental vapor-liquid equilibrium (VLE) data and allows one to predict thermodynamic properties for many binary mixtures. However, instead of the asymptotic critical exponents associated with the critical point, this model contains some effective exponents. The theoretical crossover Leung-Griffiths model with real exponents has been developed recently [3]. In the present paper, the crossover Leung-Griffiths model has been optimized to different binary mixtures: CO_2 + n-butane, CO_2 + propane, ethane + benzene, and CO_2 + methanol. Incorporation of chemical reactions in the crossover model is discussed with the example of dilute aqueous sodium chloride solutions.

2. CROSSOVER LEUNG-GRIFFITHS MODEL

The crossover Leung-Griffiths model can be represented in the form [3]:

$$\tau(\zeta) = rY(r)^{\frac{(\gamma-1)}{\Delta}}[1 - b^2\theta_s^2(r)], \tag{1}$$

$$\Delta\rho(T,\zeta) = \pm C_1(\zeta)r^{\beta}Y(r)^{\frac{(\gamma-2\beta)}{2\Delta}}\theta_s(r) + C_2(\zeta)\tau + C_5(\zeta)(-\tau)^{1-\alpha} + C_{55}(\zeta)(-\tau)^{\beta+\Delta_5}, \tag{2}$$

$$P = P_c\frac{T}{T_c}[-\Delta\bar{A} + A_0(\tau) + 1]; \qquad A_0(\tau) = \sum_{i=1}^{3} A_i\tau^i, \tag{3}$$

where the dimensionless density $\Delta\rho = \rho/\rho_c - 1$, P is the pressure, the singular part of the Helmholtz free-energy density is

$$\Delta\bar{A} = \frac{C_3(\zeta)}{a_3}r^{2-\alpha}Y(r)^{\frac{(\gamma-2\beta)}{\Delta}}[-1 + a_2\theta_s^2(r) - a_4\theta_s^4(r)] + \frac{C_4(\zeta)}{\lambda_2}\tau^2, \tag{4}$$

subscript "c" corresponds to critical values, and "$\pm$" refer to liquid (+) and to vapor (−). In Eqs. (1) - (4), critical exponents α, β, γ, Δ and Δ_5, universal constants b^2, λ_2 and a_i $(i = 1, ..., 4)$, and crossover functions $Y(r)$ and $\theta_s(r)$ are the same as in the earlier paper [3]. The independent variables of the model are

$$\zeta = 1/(K(T,\Delta\nu)e^{\Delta\nu} + 1), \qquad \tau = T/T_c - 1, \tag{5}$$

where $\Delta\nu = (\mu_2 - \mu_1)/RT$, T is the temperature, μ the chemical potential, R the gas constant and K is a function of T and $\Delta\nu$. Subscripts "1" and "2" indicate the first and second pure

components. In the present paper, unlike our previous work [3], we made a regularization to exclude the possibility of negative values of the concentrations on the vapor side of the coexistence curve. The expressions for the concentrations in the liquid and vapor read:

$$x_v = (1-\zeta)\Big/\Big[1+\zeta\Big(\frac{\bar{Q}}{\rho_v}-\frac{\bar{Q}_c}{\rho_c}+\frac{1}{T_c}\Big(\frac{dT_c}{d\zeta}\Big)\,\tau\,C_6(\zeta,\tau)\Big)\Big/\Big(1+\zeta(1-\zeta)C_7(\zeta,\tau)\Big)\Big], \quad (6)$$

$$x_l = x_v + \zeta(1-\zeta)\Big(\frac{\bar{Q}}{\rho_v}-\frac{\bar{Q}}{\rho_l}\Big)\Big/\Big(1+\zeta(1-\zeta)C_7(\zeta,\tau)\Big). \quad (7)$$

The definitions of functions $\bar{Q}$ and $\bar{Q}_c$ coincide with that in the papers [2, 3]. Equations (6) and (7) define the relationship between the measurable concentrations x_v and x_l and the "field" variable ζ on the coexistence curve. In order to use this model to compare with experimental data for the phase equilibrium in binary mixtures, one needs to define expressions for the critical locus and the mixing rules for the system-dependent parameters. Expressions for the critical locus were defined as

$$X_c(\zeta) = X_{c0}\zeta + X_{c1}(1-\zeta) + \zeta(1-\zeta)\sum_{n=0}^{7} X_n(1-2\zeta)^n, \quad (8)$$

where X_c means T_c, ρ_c or P_c loci and subscripts "$c0$" and "$c1$" correspond to pure first ($\zeta = 1$) and second ($\zeta = 0$) components of a mixture, respectively. To represent the mixing rules for the system-dependent parameters, a modified version of an isomorphic generalization of the law of corresponding states [4] was used.

3. COMPARISON WITH EXPERIMENTAL DATA

The first mixture, to which the crossover Leung-Griffiths model was optimized, is CO_2 + n-butane. A correlation of this mixture based on the modified Leung-Griffiths model was earlier performed by Rainwater and coworkers [5]. In this work, we used those results as an initial approximation to optimize the crossover Leung-Griffiths model. The values of all adjustable parameters of the model and the parameters for the critical locus were found from non-linear regression analysis. Fig. 1 represents the result of our comparison of the model with the measurements of Olds et al. [6] and Niesen [7] in $P-x$ and $P-\rho$ spaces. The picture demonstrates very good correlation to the experimental data.

The second mixture to which the crossover Leung-Griffiths model has been optimized is the CO_2 + propane mixture. For the VLE surface we obtained results very close to those

obtained earlier by Niesen and Rainwater [8]; therefore we do not show them here. Fig. 2 shows the result of the fit to the VLE data of ethane + benzene [9] in $P-T$ and $\rho-T$ spaces. Unlike the previous mixtures, this set of data is represented on isopleths. Our procedure of optimization of the model gives us the capacity to fit directly VLE data on either isotherms or isopleths. As one can see from Fig. 2, the high standards of correlations of simpler mixtures are retained. Concerning this mixture, we note that the modified Leung-Griffiths model also provides a very good fit to the experimental data [2]. However, the modified Leung-Griffiths model predicts some peculiar VLE behavior at concentrations between $x = 0.01$ and $x = 0.05$ mole fraction of benzene, so-called "double retrograde vaporization" [2]. Our calculations give no evidence of the "double retrograde vaporization" behavior for ethane + benzene mixture. The crossover Leung-Griffiths model does not demonstrate this behavior for the ethane + benzene mixture in the limit of dilute benzene, although the maxcondentherm locus shows an abrupt drop in pressure.

The fourth mixture which we represent in this work is the CO_2 + methanol mixture. Fluid mixtures containing methanol are important for optimum design and operation in the chemical industry. The phase diagrams for this mixture are more complicated than for the mixtures discussed above. The coexisting vapor-liquid isotherms in $P - x$ space are very wide and compositions at the vapor branch of the coexistence curve in the dilute methanol solutions remain small down to pressures about 50% below P_c without exhibiting so-called "bird's beak" behavior. We note that our optimization procedure allows us also to reproduce the critical locus of a mixture from a fit to the VLE data. For comparison of our model with experimental data, four different sets of experimental data have been used [10, 11, 12, 13]. These experimental data obtained on the separate isotherms are relatively sparse; therefore a determination of the critical locus for this mixtures becomes an independent task. We found the critical locus for this mixture in two steps. Firstly, we fit our model to the experimental VLE data at temperatures 315.15 K $\leq T \leq$ 423.15 K and found the critical locus in the concentration range $0 \leq x \leq 0.5$. Then we repeated this procedure at temperatures 352.60 K $\leq T \leq$ 477.60 K and found the critical locus at $0.5 \leq x \leq 1$. Secondly, we interpolated the result obtained from the previous fit critical locus data with Eq. (8) in the entire region $0 \leq x \leq 1$ and found all adjustable parameters

of the model from a fit to the complete set of experimental VLE data.

The results of our calculations in comparing with experimental critical locus data obtained by Leu et al. [13], by Gurdial et al. [14] and by Brunner and co-workers [11] are shown on Fig. 3. As one can see, the calculated $T_c - x$ and $P_c - x$ loci exhibit a minimum at concentration $x \simeq 0.04$ mole fraction of methanol, which is not observed for the only experimental data in this region obtained by Gurdial et al. [14]. These seem to be inconsistent in $P - x$ and $T - x$ coordinates with experimental data of Leu et al. [13] and of Brunner et al. [11], at higher concentration, however, in the $P - T$ space, the calculated critical locus and experimental data are fully consistent. The values of the coefficients X_n in Eq. (8) for the critical locus of binary mixtures are listed in Table I. A comparison with experimental VLE data is shown in Fig. 4. The correlation with the experimental data is poorer than in the previous cases, especially very close to pure CO_2 where the discrepancy between different sets of experimental data is observed. For a better representation of the VLE surface, more experimental data, especially for dilute methanol solutions, are needed.

4. AQUEOUS SODIUM CHLORIDE SOLUTIONS

Dilute aqueous sodium chloride solutions, as well as carbon dioxide + methanol mixtures, close to the critical point of water or CO_2 exhibit the general features of dilute binary mixtures with the more volatile first component. However, in addition, aqueous sodium chloride solutions are characterized by the presence of dissociation-association phenomena $\mathrm{NaCl} \rightleftharpoons \mathrm{Na}^+ + \mathrm{Cl}^-$. Together with the inconsistency between different sets of the critical locus experimental data, this makes the task of describing the VLE surface in these systems extremely difficult.

A chemical reaction can be incorporated in Eqs. (3) - (7) by considering the coefficients $C_3,\ C_4,\ C_6,\ C_7$ and A_i $(i = 1, 2, 3)$ as functions of $\Delta\xi$

$$C_i(\zeta, \xi) = C_i(\zeta) + (1 - \zeta) C_{i\xi} \Delta\xi, \qquad A_i(\zeta, \xi) = A_i(\zeta)(1 + (1 - \zeta) A_\xi \Delta\xi^2), \tag{9}$$

where $\Delta\xi = \xi - \xi_c(\zeta)$, the extent of the reaction ξ is determined by the expressions

$$n_{NaCl} = n^0_{NaCl} - \xi, \qquad n_{Na^+} = \xi, \qquad n_{Cl^-} = \xi, \tag{10}$$

(n is a number of moles of the components of the reaction), $0 \leq \xi_c(\zeta) \leq \xi_{max}$ is the extent of the reaction at the critical point, and $\xi_{max} = n^0_{NaCl}$ is the maximum value of ξ. At chemical

equilibrium $(\partial A/\partial \xi)_{T,\rho,\zeta} = 0$, and an asymptotic expression for the extent of the reaction in zero external field (which corresponds to the coexistence curve at $T < T_c(x)$ and to the critical isochore at $T \geq T_c(x)$) can be written in the form

$$\xi = \xi_c(\zeta) + (1-\zeta) C_{3\xi}^{\pm} r^{2-\alpha} A_0^{-1}(\tau), \tag{11}$$

where $C_{3\xi}^{\pm}$ is the asymptotic critical amplitude of the extent of the reaction above ($^+$) and below ($^-$) the critical temperature. In the zero field $r \propto |\tau|$, $A_0(\tau) \propto \tau$, and, as one can see from Eq. (11), at the critical isochore $\Delta\xi \propto |\tau|^{1-\alpha}$, which exactly corresponds to the decorated-lattice model calculations [15]. In the two-phase region at constant temperature the dimensionless temperature τ becomes a function of the field variable ζ only and, as a consequence, in the state of the chemical equilibrium all coefficients in Eqs. (3) - (7) become more complicated functions of the field variable ζ than in the non-reacting systems, and more complex expressions for the coefficients $C_3(\zeta)$, $C_6(\zeta)$ and $C_7(\zeta)$ as functions of the field variable ζ have to be used. The results of the description of the experimental phase equilibrium data for dilute solutions of NaCl in H_2O with the crossover Leung-Griffiths model, where the complex functional dependence of the coefficients $C_3(\zeta)$, $C_6(\zeta)$ and $C_7(\zeta)$ upon the field variable ζ has been already included, are presented in our previous paper [3]; therefore we will not discuss them here.

In the present work, in order to compare the model with experimental information, we applied equation (11) to the calculation of the dissociation constant K_m at the critical isochore in the supercritical region of the 0.1 mole % NaCl solution in water. Unfortunately, there is no experimental dissociation constant data at the critical isochore for the $H_2O + NaCl$ solutions; therefore, we generated them using the empirical correlation obtained by Ho et al. [16] and by Zimmerman et al. [17] from a fit to their experimental conductance data in the supercritical region of dilute aqueous sodium chloride solutions. The dissociation constant in Refs. [16, 17] is obtained from the relation

$$K_m = \epsilon^2 m \gamma_{\pm}/(1-\epsilon), \tag{12}$$

with the molality m, the degree of dissociation ϵ, and the mean activity coefficient of the free ions $\gamma_{\pm}$ calculated from the Debye-Hückel limiting law

$$\ln \gamma_{\pm} = -\kappa q_B \epsilon^{1/2}/(1+\kappa q_B \epsilon^{1/2}), \tag{13}$$

where κ is the reciprocal radius of the ionic atmosphere, and q_B is the Bjerrum distance. In the present paper for the calculation of the dissociation constant we use the same expressions; however, instead of experimental values of the degree of dissociation we use $\epsilon = \xi/\xi_{max}$ with ξ calculated with Eq. (11). The calculations were performed in two steps. Firstly, using the parametric crossover equation of state for dilute aqueous NaCl solutions [4] we calculated temperatures and pressures along the critical isochore of the 0.1 mole % NaCl solution. Then, using the analytical equation of state [19] we calculated at these values of temperatures and pressures the densities of pure water and values of the molality m corresponding to them. The values of the dielectric constant of water were obtained from the new formulation of Fernandez et al. [18] adopted by IAPWS. The result of our calculations in comparison with the data generated with these two empirical correlations is shown in Fig. 5. Since the empirical correlation of Ho et al. [16] and of Zimmerman et al. [17] differ in the critical region, we found the critical values for the extent of the chemical reaction ξ_c and the coefficient $C_{3\xi}$ for each set of generated data separately. As one can see from Fig. 5, in the temperature range 690 K $< T <$ 750 K our calculations and empirical correlation give essentially the same results. In the near-critical region at $T_c < T <$ 690 K our model and empirical correlation give qualitatively similar behavior for the dissociation constant, but quantitatively the difference between them increases. The temperatures 655 K $< T <$ 680 K correspond to the range of densities for pure water 265 $\mathrm{kg \cdot m^{-3}} < \rho_{\mathrm{H_2O}} <$ 325 $\mathrm{kg \cdot m^{-3}}$. At these densities the uncertainties between the conductance data obtained from the different literature sources are estimated to be up to 50%, and lead to the corresponding uncertainties of the dissociation constant obtained from these data (see discussions in Refs. [16, 17]). Because of the lack of experimental data at the critical isochore of the 0.1 mole % NaCl solution, we do not know which model gives a correct behavior of the dissociation constant in this region. To answer this question, both a more detailed experimental and theoretical study of the chemical reaction in the critical region of dilute sodium chloride aqueous solutions is needed.

ACKNOWLEDGMENTS

The authors are indebted to A. H. Harvey and J. M. H. Levelt Sengers for valuable

discussions and constructive comments. Two of us (M.Yu.B. and S.B.K.) would like to thank the Physical and Chemical Properties Division, National Institute of Standards and Technology for the opportunity to work as Guest Researchers at NIST during the course of this research.

REFERENCES

[1] S.S. Leung and R.B. Griffiths, Phys. Rev. A, 8 (1973) 2673.

[2] J. C. Rainwater, in J. F. Ely and T. J. Bruno (Eds.), Supercritical Fluid Technology, CRC Press, Boca Raton FL, 1991, p. 57.

[3] M.Yu. Belyakov, S.B. Kiselev, and J.C. Rainwater, J. Chem. Phys., in press.

[4] S. B. Kiselev, Fluid Phase Equilibria, 128 (1997) 1.

[5] J. C. Rainwater, H. Ingham, and J. J. Lynch, J. Res. Natl. Inst. Stand. Technol., 95 (1990) 701.

[6] R. H. Olds, H. H. Reamer, B. H. Sage, and W. N. Lacey, Ind. Eng. Chem., 41 (1949) 475.

[7] V. G. Niesen, J. Chem. Thermodynamics, 21 (1989) 915.

[8] V. G. Niesen and J. C. Rainwater, J. Chem. Thermodynamics, 22 (1990) 777.

[9] W. B. Kay and T. D. Nevens, Chem. Eng. Prog. Symp. Ser., 48(3) (1952) 108.

[10] K. Ohgaki and T. Katayama, J. Chem. Eng. Data, 21 (1976) 53.

[11] E. Brunner, W. Hültenschmidt, and G. Schlichthärle, J. Chem. Thermodynamics, 19 (1987) 273.

[12] K. Suzuki, H. Sue, M. Itou, R. L. Smith, H. Inomata, K. Arai, and S. Saito, J. Chem. Eng. Data, 35 (1990) 63.

[13] A.-D. Leu, S. Y.-K. Chung, and D. B. Robinson, J. Chem. Thermodynamics, 23 (1991) 979.

[14] G. S. Gurdial, N. R. Foster, S. L. J. Yun, and K. D. Tilly, in E. Kiran and J. F. Brennecke (Eds.), Supercritical Fluid Engineering Science: Fundamentals and Applications, Am. Chem. Soc., Washington, DC, 1993, p. 34.

[15] J. C. Wheeler and R. G. Petschek, Phys. Rev. A, 28 (1983) 2442.

[16] P.C. Ho, D.A. Palmer, and R.E. Mesmer, J. Solution Chem., 23 (1994) 997.

[17] G.H. Zimmerman, M.S. Gruszkiewich, and R.H. Wood, J. Phys. Chem., 99 (1995) 11612.

[18] D. P. Fernandez, A. R. H. Goodwin, E. M. Lemmon, J. M. H. Levelt Sengers, and R. C. Williams, J. Phys. Chem. Ref. Data, in press.

[19] P. G. Hill, J. Phys. Chem. Ref. Data, 19 (1990) 1233.

Table I: Critical-Line Parameters for Carbon Dioxide + n-Butane, Carbon Dioxide + Propane, Ethane + Benzene and Carbon Dioxide + Methanol mixtures (T in K, ρ in $\mathrm{mol \cdot L^{-1}}$, P in MPa).

Critical parameters	CO_2+ n-butane	CO_2+ propane	C_2H_6+ benzene	CO_2+ methanol
T_{c0}	304.12164	304.12164	305.322	304.12164
T_0	53.59122	-14.54966	178.33226	53.49050
T_1	-20.91389	-33.81628	31.47648	-129.76893
T_2	-50.59992	-20.70175	-56.56226	-60.55495
T_3	-55.19490	0	0	204.43309
T_4	7.59110	-14.58828	42.84826	14.16343
T_5	56.70422	-46.57021	-55.91465	-557.11113
T_6	0	0	0	-226.72420
T_7	0	0	0	124.29954
T_{c1}	425.16	369.95778	561.75	512.60
ρ_{c0}	10.63849	10.63849	6.88972	10.63849
ρ_0	-4.94274	-4.00035	1.59630	-
ρ_1	-0.55389	-0.79376	5.57374	-
ρ_2	-0.49891	0.40147	2.75355	-
ρ_3	-1.78224	0	-4.01097	-
ρ_4	-3.82475	-11.40505	8.38512	-
ρ_5	-2.16191	-9.07678	2.10400	-
ρ_6	0	0	0	-
ρ_7	0	0	0	-
ρ_{c1}	3.9494	5.00070	3.85966	8.50161
P_{c0}	7.37483	7.37483	4.8718	7.37483
P_0	7.44059	2.13141	17.51390	35.42662
P_1	4.65992	-1.49720	14.58651	9.95831
P_2	-2.21491	-0.88143	1.09140	-19.32461
P_3	-7.08479	1.99192	-7.56474	20.66151
P_4	-1.82780	-7.12581	0	-44.70212
P_5	3.49655	-11.56558	-2.27877	-151.16455
P_6	0	0	0	24.62120
P_7	0	0	0	115.51089
P_{c1}	3.79264	4.24831	4.87575	8.0970

FIGURE CAPTIONS

Fig. 1. VLE isotherms for CO_2 + n-butane from the model (solid curves) as compared with the experimental data of Olds et al. [6] (filled) and of Niesen [7] (empty).

Fig. 2. Coexistence surface and crossover Leung-Griffiths correlation (solid curves) for ethane + benzene, with the experimental data (symbols) from Ref. [9]. Also shown is the calculated dew-bubble curve for 3% benzene with earlier model [2] (dotted line) and present model (dashed line).

Fig. 3. The critical locus of CO_2 + methanol mixture as predicted by crossover Leung-Griffiths model (solid curves) in comparison with the experimental data of Brunner et al. [11], of Leu et al. [13] and of Gurdial et al. [14].

Fig. 4. Pressure-composition diagram for CO_2 + methanol. Solid curves correspond to the model and symbols indicate the experimental data of Ohgaki et al. [10], of Brunner et al. [11], of Suzuki et al. [12] and of Leu et al. [13].

Fig. 5. The dissociation constants K_m of 0.1 mole % NaCl aqueous solution as functions of temperature along the critical isochore. The symbols indicate values calculated with the empirical correlation of Ho et al. [16] (filled) and of Zimmerman et al. [17] (empty), and the curves represent values calculated with Eqs. (11) - (13).

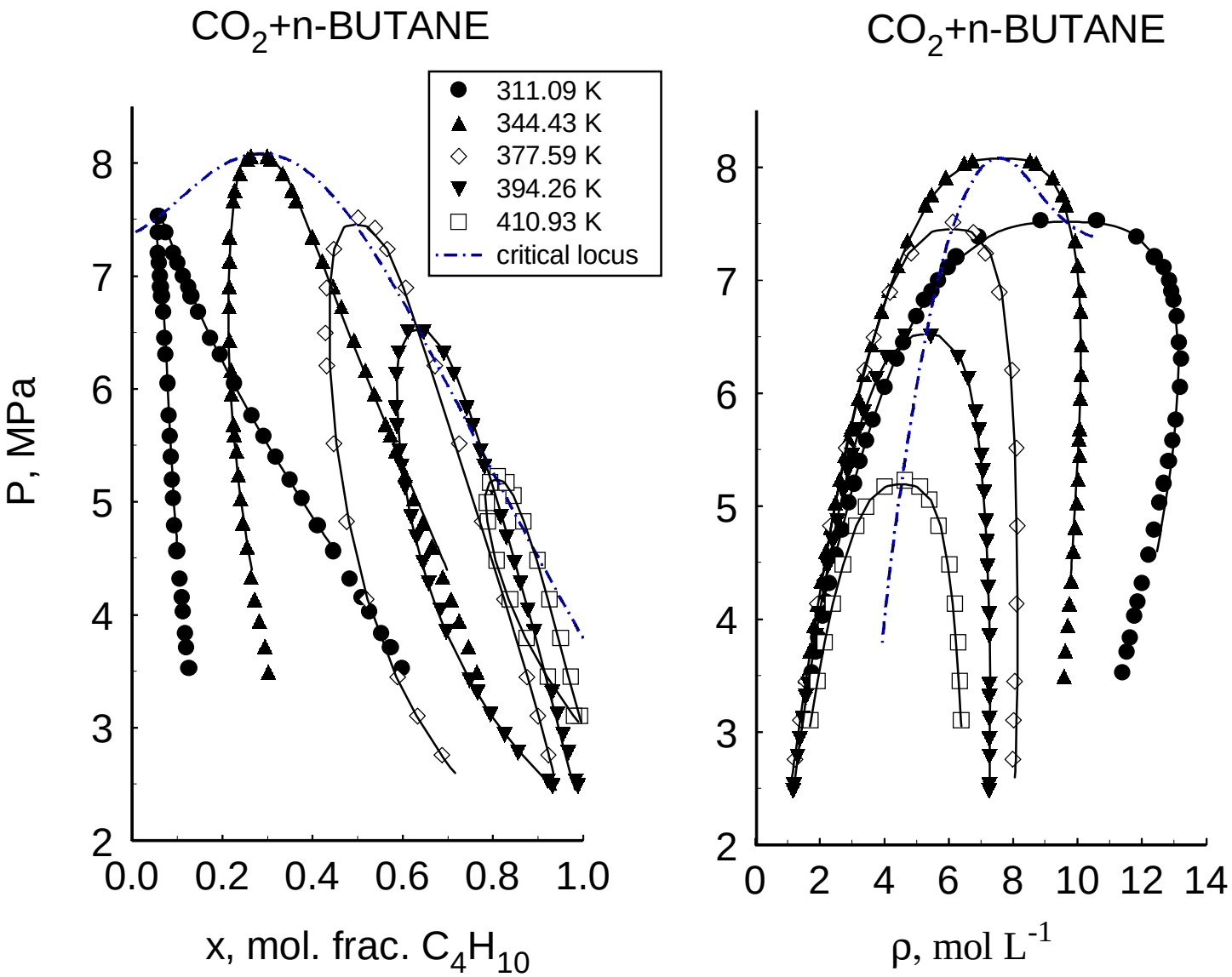
CO2+n-BUTANE
311.09 K
344.43 K
377.59 K
394.26 K
410.93 K
critical locus
P, MPa
x, mol. frac. C4H10
CO2+n-BUTANE
ρ, mol L-1

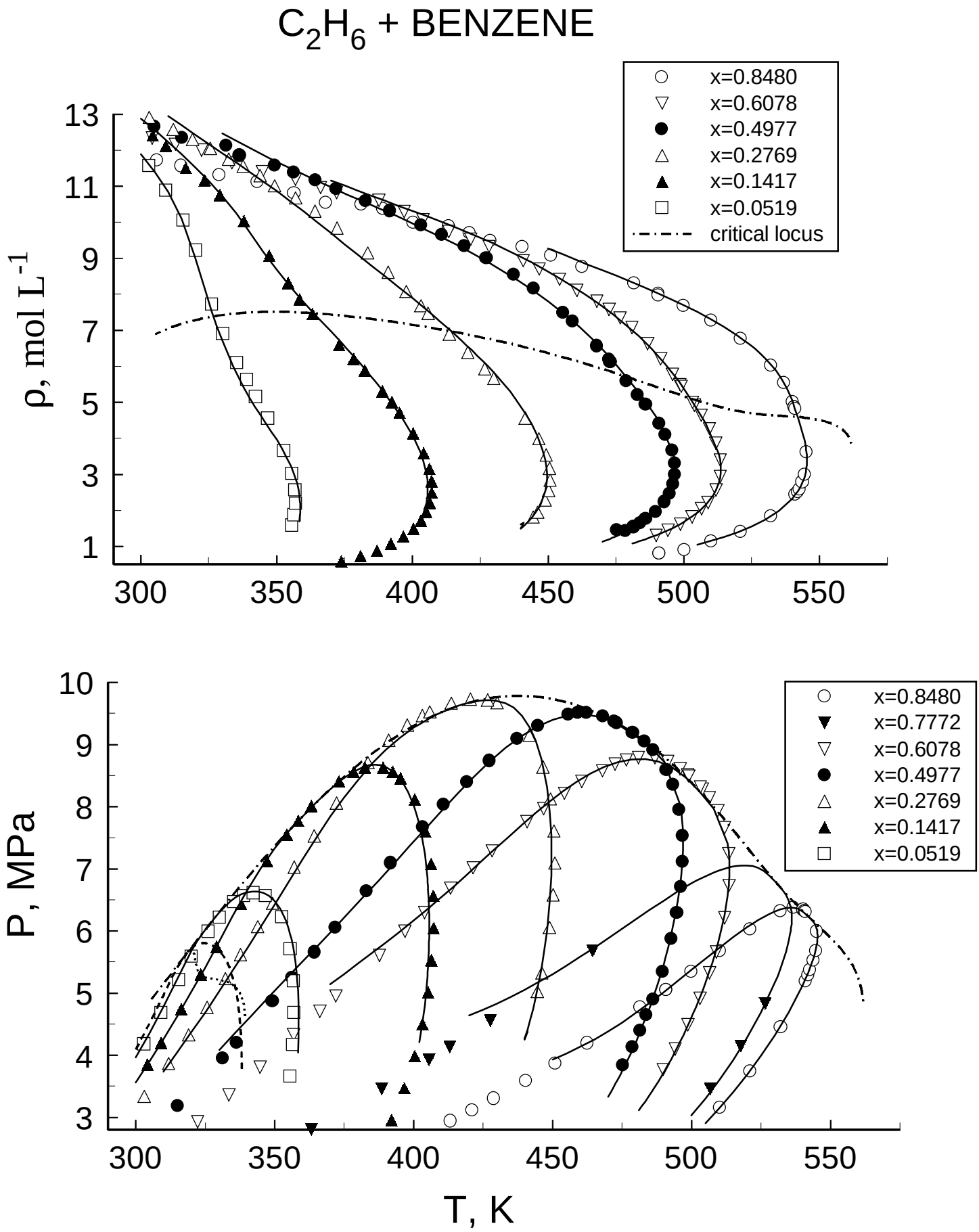
C2H6 + BENZENE
x=0.8480
x=0.6078
x=0.4977
x=0.2769
x=0.1417
x=0.0519
critical locus
ρ, mol L-1
13
11
9
7
5
3
1
300
350
400
450
500
550
x=0.8480
x=0.7772
x=0.6078
x=0.4977
x=0.2769
x=0.1417
x=0.0519
P, MPa
10
9
8
7
6
5
4
3
300
350
400
450
500
550
T, K

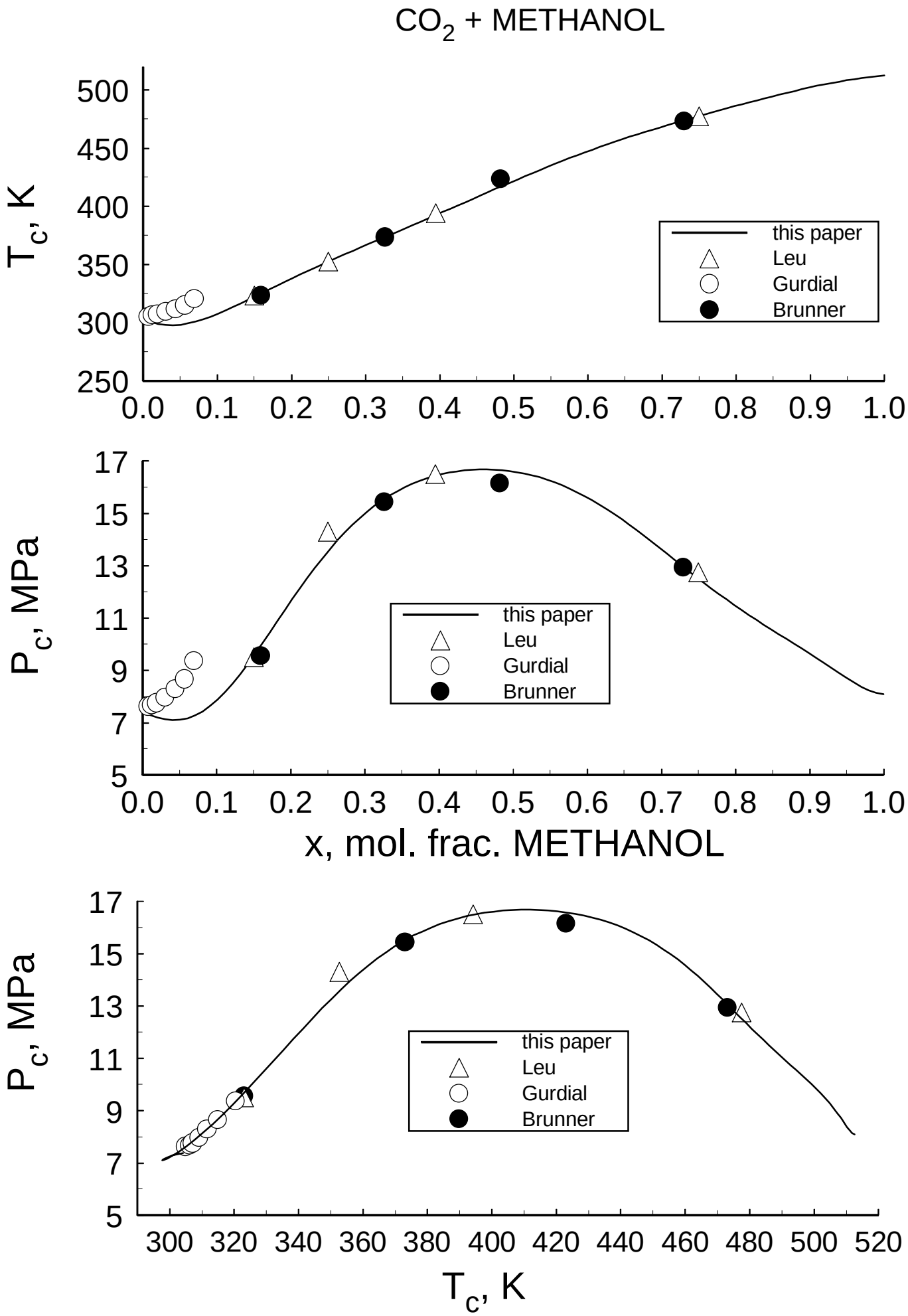
CO2 + METHANOL
Tc, K
500
450
400
350
300
250
0.0
0.1
0.2
0.3
0.4
0.5
0.6
0.7
0.8
0.9
1.0
this paper
Leu
Gurdial
Brunner
Pc, MPa
17
15
13
11
9
7
5
x, mol. frac. METHANOL
Pc, MPa
Tc, K
300
320
340
360
380
400
420
440
460
480
500
520

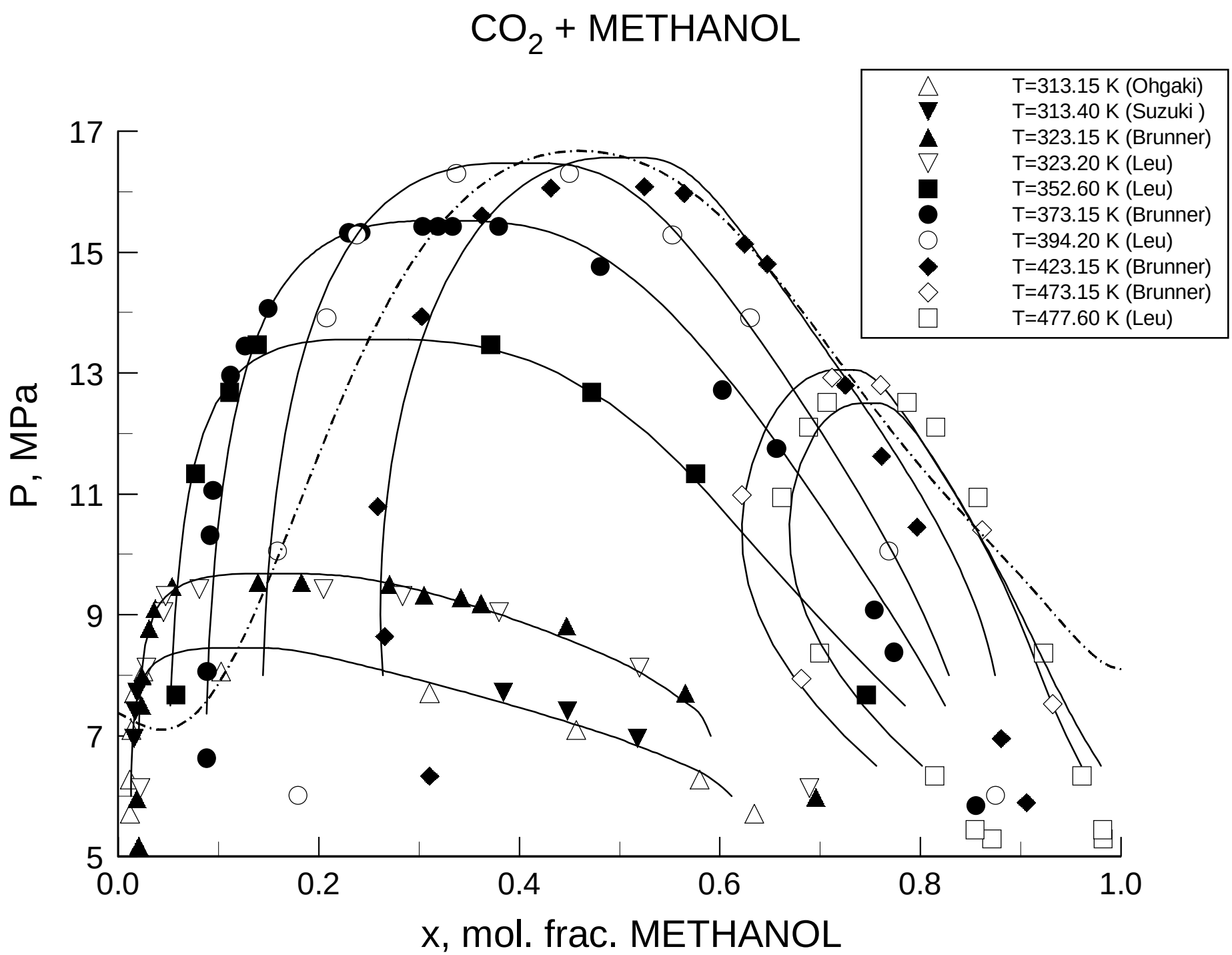
CO2 + METHANOL
T=313.15 K (Ohgaki)
T=313.40 K (Suzuki)
T=323.15 K (Brunner)
T=323.20 K (Leu)
T=352.60 K (Leu)
T=373.15 K (Brunner)
T=394.20 K (Leu)
T=423.15 K (Brunner)
T=473.15 K (Brunner)
T=477.60 K (Leu)
P, MPa
17
15
13
11
9
7
5
0.0
0.2
0.4
0.6
0.8
1.0
x, mol. frac. METHANOL

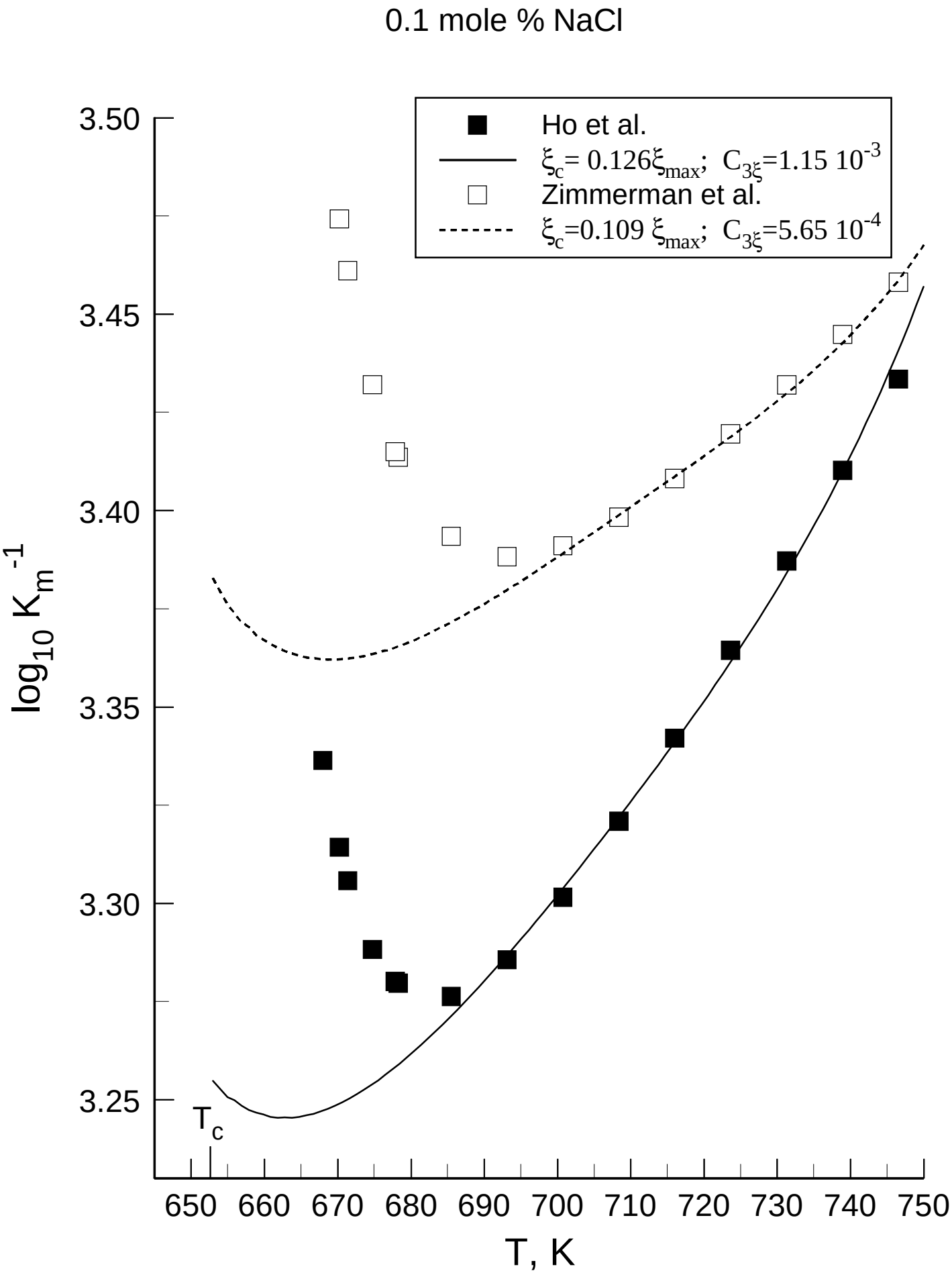
0.1 mole % NaCl
Ho et al.
ξ_c= 0.126ξ_{max}; $C_{3\xi}$=1.15 10^{-3}
Zimmerman et al.
ξ_c=0.109 ξ_{max}; $C_{3\xi}$=5.65 10^{-4}
3.50
3.45
3.40
3.35
3.30
3.25
$\log_{10} K_m^{-1}$
T_c
650
660
670
680
690
700
710
720
730
740
750
T, K